Density-functional study of the thermodynamic properties and the pressure–temperature phase diagram of Ti

Zhi-Gang Mei, Shun-Li Shang, Yi Wang, and Zi-Kui Liu
Materials Science and Engineering, Pennsylvania State University, University Park, Pennsylvania 16802, USA
(Received 8 June 2009; revised manuscript received 24 August 2009; published 24 September 2009)

The phonon spectra of α, β, and ω Ti were studied using the supercell approach. The lattice vibrational energy was calculated in the quasiharmonic approximation using both first-principles phonon density of state and Debye model. The thermal electronic contribution to the free energy was evaluated from the integration over the electronic density of states. The Helmholtz energy was thus obtained by combining them with the 0 K total energy calculated within the framework of all-electron projector-augmented-wave method. The thermodynamic properties of α and ω Ti calculated by phonon and Debye model are very close to each other. The predicted enthalpy, entropy, bulk modulus, thermal expansion coefficient and heat capacity of α are in good agreement with experiments. By comparing with the experimental enthalpy of β, we found that the 0 K total energy calculated from bcc Ti is incorrect. This problem can be solved by shifting the total energy of β down by 8 kJ mol^{-1} to match the experimental value. With the Gibbs energy calculated from the Debye model as a function of pressure and temperature, the phase transformation conditions of $\alpha \rightarrow \omega$, $\alpha \rightarrow \beta$, and $\beta \rightarrow \omega$ were identified. The predicted transition temperature between α and β at ambient pressure and the triple point are close to experiments. It was found that the entropy plays an important role in the $\omega \rightarrow \alpha$ and $\alpha \rightarrow \beta$ transitions, and the thermal electronic contribution to the Gibbs energy cannot be neglected for studying the $\alpha \rightarrow \beta$ transition. Our calculations also showed that zero-point energy is crucial to predict the transition pressure of Ti at low temperatures.

DOI: 10.1103/PhysRevB.80.104116 PACS number(s): 64.70.K−, 65.40.−b, 63.20.D−, 61.50.Ah

I. INTRODUCTION

In the past decade, Ti has attracted tremendous interests due to its technological and scientific importance. It has been widely studied both experimentally and theoretically. There are five solid phases of Ti reported in the literature: α (hcp), β (bcc), ω (hexagonal), γ (distorted hcp), and δ (distorted bcc).[1–4] γ and δ are two recently discovered high-pressure phases.[2,3] Extensive experimental studies of the pressure-induced phase transition $\alpha \rightarrow \omega$ show a large hysteresis. At room temperature, the accepted equilibrium transition pressure of 2.0 ± 0.3 GPa was estimated from measurements of shear stressed samples because the shear reduces the hysteresis.[5] At ambient pressure, with increasing temperature, α transforms to the high-temperature phase β at 1155 K.[6] The transitional temperature decreases as the pressure increases, stabilizing the high-temperature β phase.

First-principles calculations have also been widely used to understand the phase stability of Ti.[7–16] In our recent work,[14] we have further clarified the 0 K phase transition sequence of Ti as $\alpha \rightarrow \omega \rightarrow \gamma \rightarrow \beta$. Among these studies, most of them are focused on the 0 K phase stability. Only a few have studied the temperature effect on the phase transitions. Rudin *et al.*[13] investigated the temperature and pressure dependence of $\alpha \rightarrow \omega$ transition using a tight-binding model based on first-principles calculations, while Hao *et al.*[7] explored the same problem using the Debye model. However, the complete pressure-temperature (P-T) phase diagram of Ti has not been well studied due to the well-known unstable phonon modes of the β phase at low temperatures.[17] Ostanin and Trubitsin[15] first worked on the P-T phase diagram of α, β, and ω Ti using the Debye model. The fitting parameters of the ω phase used in the Debye model, however, was obtained without detailed justifications.[15] Recently, Hennig *et al.*[16] studied the P-T phase diagram of Ti using molecular-dynamics simulations based on modified embedded atom potential. Their prediction that the transition temperature between α and β is nearly independent of the pressure does not agree with the experimental results.[6]

In this paper, utilizing the quasiharmonic approximation, we predicted the thermodynamics properties of α and ω Ti from the first-principles phonon density of state (DOS). The Debye model was explored in calculating the lattice vibrational energy and predicting the complete P-T phase diagram of α, β, and ω Ti. The γ phase is not included in the present study of the P-T phase diagram due to its extremely narrow stable range at high pressures.[14]

The rest of the paper is organized as follow. The theory of Helmholtz energy calculation in the quasiharmonic approximation is briefly introduced in Sec. II. The computational details of first-principles and phonon spectra calculations are described in Sec. III. The predictions of the thermodynamic properties and P-T phase diagram of Ti are discussed in Sec. IV. Finally, we give a summary of this work in Sec. V.

II. THEORY

The Helmholtz energy F at volume V and temperature T can be approximated as[18,19]

$$F(V,T) = E(V) + F_{vib}(V,T) + F_{ele}(V,T), \quad (1)$$

where E is the 0 K total energy, F_{vib} the vibrational energy of the lattice ions, and F_{ele} the thermal electronic contribution to the free energy.

Under quasiharmonic approximation, F_{vib} can be calculated from phonon DOS by[20]

$$F_{\mathrm{vib}}(V,T) = k_{\mathrm{B}}T\int_0^{\infty} \ln\left\{2\sinh\left[\frac{\hbar\omega}{2k_{\mathrm{B}}T}\right]\right\} g(\omega,V)d\omega, \quad (2)$$

where ω represents the phonon frequency, and $g(\omega,V)$ the phonon DOS at frequency ω and volume V. For mechanically unstable phases, however, F_{vib} cannot be evaluated using Eq. (2) due to the imaginary phonon frequencies. Instead, it can be estimated from the empirical Debye model[21]

$$F_{\mathrm{vib}}(V,T) = \frac{9}{8}k_{\mathrm{B}}\Theta_{\mathrm{D}} + k_{\mathrm{B}}T\left\{3\ln\left[1-\exp\left(-\frac{\Theta_{\mathrm{D}}}{T}\right)\right] - D\left(-\frac{\Theta_{\mathrm{D}}}{T}\right)\right\} \quad (3)$$

where $\frac{9}{8}k_{\mathrm{B}}\Theta_{\mathrm{D}}$ is zero-point energy due to lattice ion vibration at 0 K, and $D(\Theta_{\mathrm{D}}/T)$ the Debye function given by $D(x) = 3/x^3\int_0^x t^3/[\exp(t)-1]dt$. It is crucial to obtain the Debye temperature Θ_{D} in order to evaluate Eq. (3). Based on Debye-Grüneisen approximation, Θ_{D} can be described as[21]

$$\Theta_{\mathrm{D}} = sAV_0^{1/6}\left(\frac{B_0}{M}\right)^{1/2}\left(\frac{V_0}{V}\right)^{\gamma} \quad (4)$$

where s is a scaling factor with $s=0.617$ obtained by Moruzzi *et al.*[21] for nonmagnetic cubic metals, A a constant, V_0 the equilibrium volume, B_0 the equilibrium bulk modulus, M the atomic mass, and γ the Grüneisen constant.

F_{ele} is obtained from the energy and entropy contributions, i.e., E_{ele}-TS_{ele}.[18] The electronic entropy S_{ele} takes the form[18]

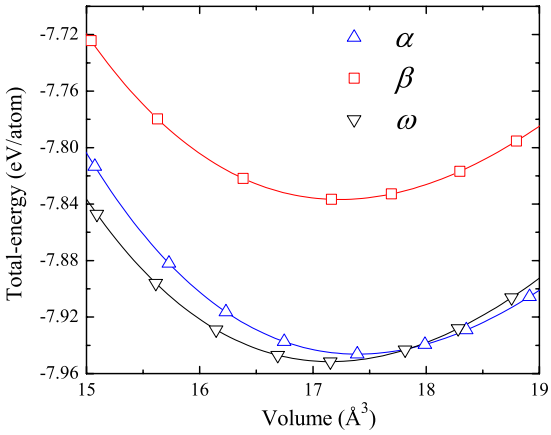

FIG. 1. (Color online) Zero kelvin total energy (E) of α, β, and ω Ti as a function of volume per atom. Open symbols are direct calculation results by VASP. Solid lines are fitted E-V curves according to the third-order Burch-Murnaghan EOS.

$$S_{\mathrm{ele}}(V,T) = -k_{\mathrm{B}}\int n(\varepsilon,V)[f\ln f + (1-f)\ln(1-f)]d\varepsilon, \quad (5)$$

where $n(\varepsilon)$ is the electronic DOS with f being the Fermi-Dirac distribution. The energy E_{ele} due to the electron excitations can be expressed as[18]

TABLE I. Equilibrium properties of Ti phases.

Phase	Reference	Temperature (K)	c/a	V_0 (Å^3/atom)	B_0 (GPa)	B_0'
α	This work	0	1.583	17.39	111.4	3.5
	This work[a]	300	1.583	17.54	106.5	3.5
	Expt. (Ref. 29)	300	1.586	17.64	114.0 ± 3.0	4.0
	Expt. (Ref. 30)	300	1.583	17.70 ± 0.05	117.0 ± 9.0	3.9 ± 0.4
	Expt. (Ref. 2)	300	1.585	17.74	102.0	3.9
	Expt. (Ref. 31)	300			109.0	3.4
ω	This work	0	0.618	17.16	111.5	3.5
	This work[a]	300	0.618	17.30	106.7	3.5
	Expt. (Ref. 29)	300	0.613	17.29	107.0 ± 3.0	4.0
	Expt. (Ref. 3)	300	0.608	17.37	123.1 ± 4.7	3.2 ± 1.2
	Expt. (Ref. 2)	300	0.614	17.37	142.0	3.9
	Expt. (Ref. 30)	300	0.609	17.40 ± 0.08	138.0 ± 10.0	3.8 ± 0.5
β	This work	0	1.000	17.24	106.3	3.3
	This work[b]	1270	1.000	18.13	94.4	3.3
	Expt. (Ref. 4)	1273	1.000	18.13	87.7	
	Expt. (Ref. 17)	1293	1.000	18.22	118	

[a]Calculated using phonon DOS.
[b]Calculated using Debye model.

$$E_{\text{ele}}(V,T) = \int n(\varepsilon,V) f \varepsilon d\varepsilon - \int_0^{\varepsilon_F} n(\varepsilon,V)\varepsilon d\varepsilon, \qquad (6)$$

where ε_F is the Fermi energy.

III. COMPUTATIONAL DETAILS

Density-functional calculations within the generalized gradient approximation (GGA), as implemented in Vienna *ab initio* simulation package (VASP),[22,23] were utilized in this study. Perdew-Burke-Ernzerhof GGA (Ref. 24) for the exchange-correlation potential was used for all calculations. The all-electron projector-augmented-wave method[25] was adopted. Dense k-point samplings in the first Brillouin zone were utilized, i.e., $36\times36\times32$ for α, $32\times32\times32$ for β, and $24\times24\times32$ for ω. Accurate total energy calculations were performed by means of the linear tetrahedron method with Blöchl's correction.[26] In all cases the total energies were converged to 10^{-8} eV/cell with a 500 eV plane wave cutoff energy.

Phonon frequency calculations were carried out in the framework of the supercell approach using small displacement method as implemented in the FROPHO code.[27] To maintain the high accuracy indicated above we used $3\times3\times3$ supercells for α, $4\times4\times4$ for β, and $3\times3\times3$ for ω, respectively. The forces induced by small displacements were calculated using VASP.

IV. RESULTS AND DISCUSSIONS

A. Atomic structure and static energy

We calculated the total energy (E) of α, β, and ω Ti at 15 different volumes (V), which are fitted by the third-order Birch-Murnaghan equation[14,28] to obtain the 0 K equilibrium properties. Figure 1 shows the calculated total energy for α, β, and ω Ti as a function of volume per atom. As indicated in Fig. 1, the ω phase has the lowest total energy at 0 K. The calculated equilibrium properties c/a ratio, atomic volume (V_0), isothermal bulk modulus (B_0), and first derivative of bulk modulus with respect to pressure (B_0') at 0 K are shown in Table I together with the predicted equilibrium properties at finite temperatures. The calculated c/a ratios of α and ω agree very well with experiments.[2,29–31] The predicted equilibrium volumes at 0 K are smaller than the experimental data[2,29,30] measured at finite temperatures. After considering the temperature effect, the calculated atomic volumes of α and ω at 300 K and β at 1270 K agree much better with experiments.[2,29,30] The bulk modulus is calculated according to the formula $B_0 = V_0(\frac{\partial^2 F}{\partial V^2})_{V_0}$, and compares well with experimental data.[2,29–31]

B. Phonon dispersion

In Fig. 2, we show the calculated phonon dispersion curves and phonon DOS of α, β, and ω Ti at experimental volumes, i.e., 17.64 Å^3/atom at 298 K,[29] 18.22 Å^3/atom at 1300 K,[17] and 17.37 Å^3/atom at 298 K,[2] respectively. We compared the phonon dispersion results of α with the inelastic neutron-scattering measurement by Stassis *et al.*[32] The agreement looks better than other theoretical predictions,[16,33] which can be due to our more accurate force calculations. At the K point, the calculated optical frequencies show the largest deviations from experiment, which also appears in others' calculations.[16,33] For high-pressure ω phase, there is no experimental phonon data to compare yet. The high-temperature β phase is mechanically unstable at low temperatures and shows soft modes in the experimental data for

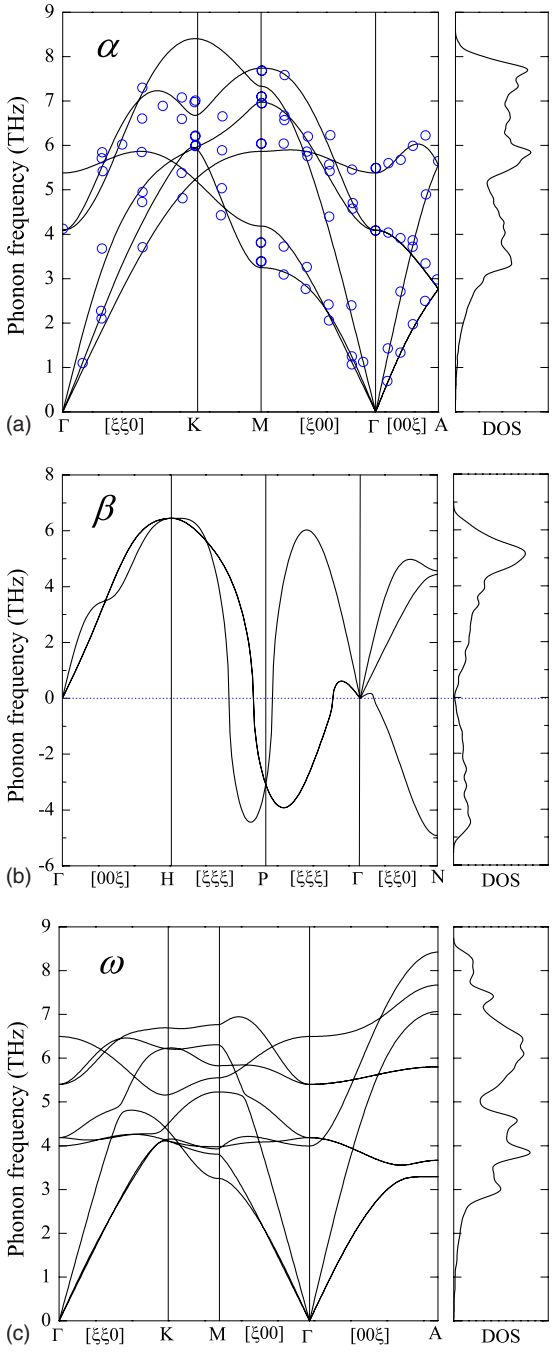

FIG. 2. (Color online) Phonon dispersion curves of α, β, and ω Ti are plotted as solid lines using experimental volumes 17.64 Å^3/atom at 298 K (Ref. 29), 18.22 Å^3/atom at 1300 K (Ref. 2), and 17.37 Å^3/atom at 298 K (Ref. 17), respectively. The calculated phonon results of α Ti are compared with the experimental data measured by Stassis *et al.* (Ref. 32) (open circles).

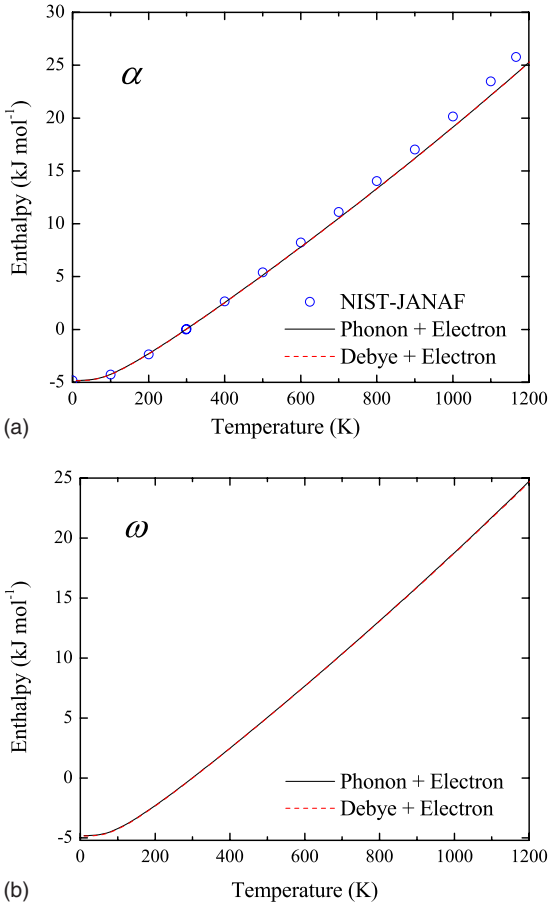

FIG. 3. (Color online) Enthalpy (H) of α and ω Ti as a function of temperature. The calculated results using phonon DOS and Debye model are plotted as solid and dashed lines, respectively. The experimental data from NIST-JANAF (Ref. 35) are plotted as open circles.

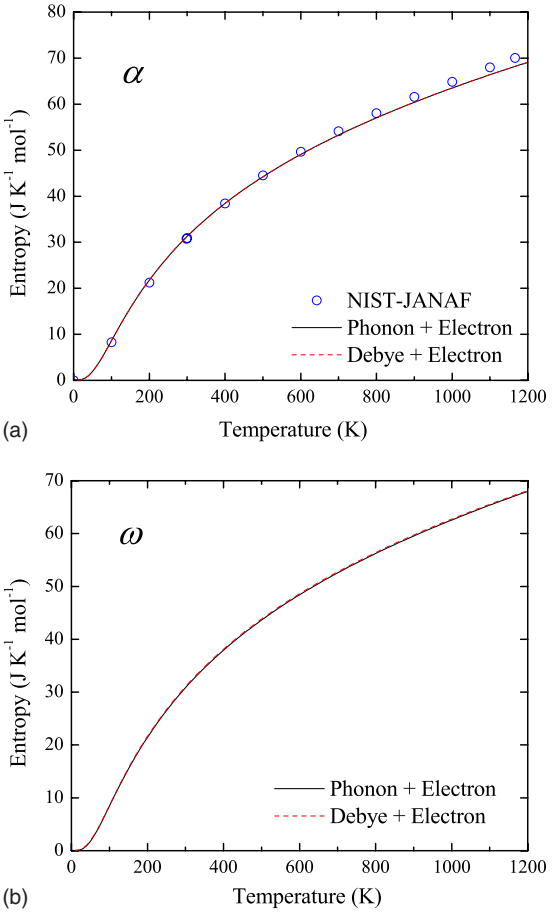

FIG. 4. (Color online) Entropy (S) of α and ω Ti as a function of temperature. The calculated results using phonon DOS and Debye model are plotted as solid and dashed lines, respectively. The experimental data from NIST-JANAF (Ref. 35) are plotted as open circles.

the $L-\frac{2}{3}[111]$ and $T-\frac{1}{2}[110]$ phonons.[17] The predicted 0 K phonon results reflect this instability showing these unstable phonon branches. $L-\frac{2}{3}[111]$ is responsible for the $\beta\rightarrow\omega$ phase transformation, while $T-\frac{1}{2}[110]$ corresponds to the $\beta\rightarrow\alpha$ phase transformation.[17] Based on the calculated phonon DOS, the Debye temperature can be estimated.[34] The Debye temperature of α is predicted to be 359 K, which agrees very well with the high-temperature limit of Debye temperature 360 K estimated by Petry *et al.*[17] For the ω phase, the Debye temperature is predicted to be 383 K.

C. Thermodynamic properties

Using the quasiharmonic approximation, we calculated the enthalpy (H), entropy (S), bulk modulus (B), linear thermal expansion coefficient (α_l), and heat capacity at constant pressure (C_P) of α and ω using both phonon DOS and Debye model. As shown in Figs. 3 and 4, the enthalpy and entropy calculated by phonon DOS are almost identical to those obtained using the Debye model for both α and ω phases. The predicted enthalpy and entropy of α are in good agreement with the experimental data from NIST-JANAF.[35] The enthalpy difference of α is within 5.6% at 1100 K, while the entropy difference of α is within 2.4% at 1100 K. Figure 5 shows the bulk modulus of α and ω as a function of temperature together with experimental data.[4,36] For both α and ω, the bulk modulus calculated by Debye model are higher than those by phonon DOS, and the difference becomes larger at higher temperature. The experimental data of α lie between those predicted by phonon DOS and Debye model. The calculated bulk modulus of α by Debye model is higher than that of Ogi *et al.*[4] by 4.5% at 1100 K. The linear thermal expansion coefficient can be evaluated by $\frac{1}{3V}[\frac{\partial V}{\partial T}]_P$. Figure 6 shows the calculated linear thermal expansion coefficient of α and ω as a function of temperature together with the experimental data assessed by Touloukian *et al.*[37] The linear thermal expansion coefficients calculated by phonon DOS and Debye model are very close with each other. The calculated results agree well with the experimental data, with difference within 4.9% at 1155 K. The heat capacity at constant volume C_V can be directly calculated by $T[\frac{\partial S}{\partial T}]_V$, while C_P can be evaluated using the thermodynamic relationship between C_V and C_P such as $C_P-C_V=(3\alpha_l)^2VBT$. As shown in Fig. 7, the calculated C_P using phonon DOS and Debye model are very close to each other for both α and ω phases. The predicted C_P of α are in good agreement with the experimental data[35,38–40] below 200

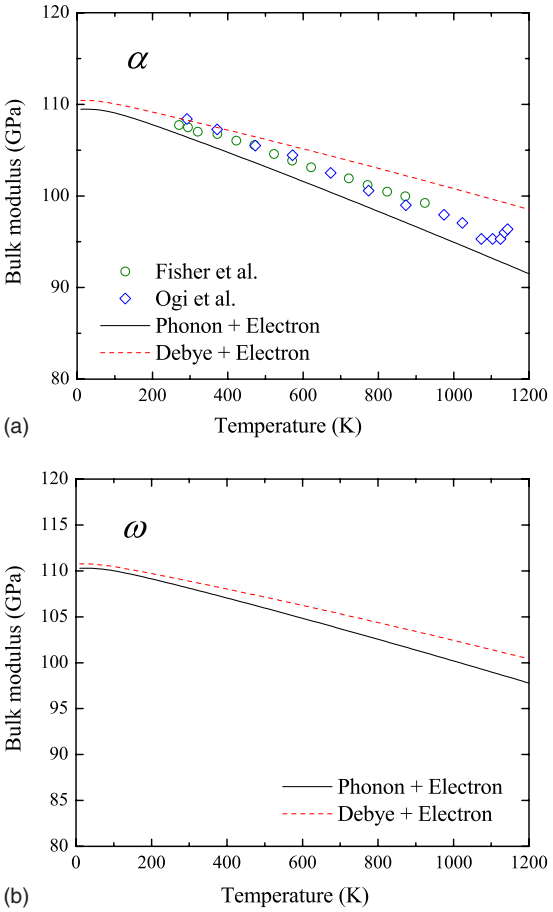

FIG. 5. (Color online) Bulk modulus (B) of α and ω Ti as a function of temperature. The calculated results using phonon DOS and Debye model are plotted as solid and dashed lines, respectively. The experimental data (Refs. 4 and 36) are plotted as open symbols.

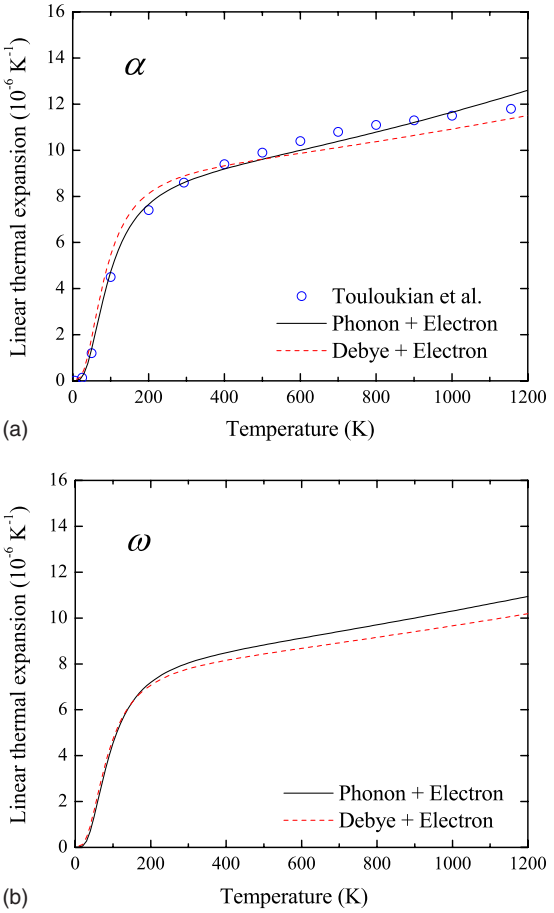

FIG. 6. (Color online) Linear thermal expansion coefficient (α_l) of α and ω Ti as a function of temperature. The calculated results using phonon DOS and Debye model are plotted as solid and dashed lines, respectively. The experimental data (Refs. 4 and 36) are plotted as open circles.

K. Above 200 K, our results are smaller than experiments by Chase[35] and Bendick and Pepperhoff.[39] Comparing with the results obtained from phonon, we found that the Debye model is a quite reliable method to investigate the thermodynamic properties of Ti phases.

As mentioned above, the phonon modes of β have imaginary frequencies, which prevent us from calculating the free energy using the phonon results directly. As an alternative approach, the thermodynamic properties of β can be studied by the Debye model. As shown in Fig. 8, the predicted entropy agrees with experiment very well. The calculated entropies are within the experiment by 1.8%. For the enthalpy, our predicted results are shifted about 8 kJ mol^{-1} above those from NIST-JANAF.[35] These energy differences come from the incorrect 0 K total energy of β calculated, which can be attributed to the oversimplified structure chosen for 0 K total-energy calculations.[41] We notice that by shifting the predicted enthalpy down by about 8 kJ mol^{-1}, the calculated enthalpy would be in a perfect agreement with experiment (see Fig. 9). The correct 0 K total energy of β might be obtained by direct *ab initio* molecular dynamics (AIMD) simulations, as recently demonstrated by Ozolins[42] who utilized this approach to predict the free energy of the unstable fcc W phase. Instead of applying the AIMD approach, we simply adjusted the 0 K total energy of β to tackle the problem in this work. As shown in the next section, the predicted P-T phase diagram of Ti agrees quite well with experiment, which further confirms our approach is feasible.

D. P-T phase diagram

The Gibbs energy (G) can be evaluated according to the formula, $G(T,P)=F(T,V)+PV$. Figure 10 shows the Gibbs energy of α, β and ω Ti as a function of temperature at different pressures, i.e., 0 GPa, 5 GPa, 11.1 GPa and 20 GPa. For $P=0$ GPa, the ω phase has the lowest Gibbs energy for the range of $0<T<186$ K; from 186 to 1114 K, the α phase is preferred, while at $T>1114$ K the β phase becomes stable. At $P=11.1$ GPa, the three phases has the same Gibbs energy at $T=821$ K, which corresponds to a triple point of the P-T phase diagram. For $P=20$ GPa, the α phase has higher Gibbs energy than the ω and β phases at all temperatures, and ω thus transforms to β without the formation of α. Comparison of the Gibbs energies as a function of pressure and temperature allows us to identify the phase transformation conditions. A similar approach has been used by Wang *et al.*[43] to predict the T-V phase diagram of Ce successfully.

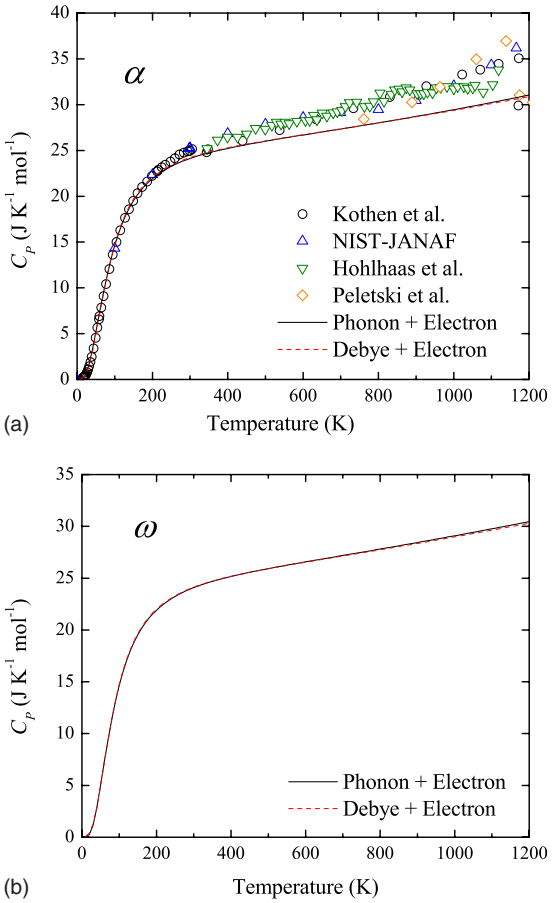

FIG. 7. (Color online) Heat capacity (C_P) of α and ω Ti as a function of temperature. The calculated results using phonon DOS and Debye model are plotted as solid and dashed lines, respectively. The experimental data (Refs. 35 and 38–40) are plotted as open symbols.

Figure 11 shows the predicted P-T phase diagram of Ti together with the experimental data.[6] The calculated $\alpha \rightarrow \beta$ transition temperature at ambient pressure is 1114 K. It compares well with the experimental value of 1155 K. The predicted transition pressure between α and ω at room temperature is 1.8 GPa, close to the experimental transition pressure 2.0 ± 0.3 GPa.[5] We also predicted a triple point (11.1 GPa, 821 K) which is also close to the experimental data (9 GPa, 940 K).[6]

To further understand the factors leading to the $\omega \rightarrow \alpha$ and $\alpha \rightarrow \beta$ transitions at zero pressure, we compared the Enthalpy and entropy differences of Ti phases as a function of temperature with respect to α, with and without the thermal electronic contribution (see Fig. 12). As we can see in Fig. 12, the enthalpy of ω is lower than that of α at all temperatures, while the enthalpy of β is always higher than that of α. As for entropy, ω has lower entropy than that of α at all temperatures, while β always has higher entropy than that of α. Since G equals to H-TS, ω becomes more and more unstable compared with α with increasing temperatures, while β becomes more and more stable with respect to α as temperature increases. It is the change in entropy that makes the $\omega \rightarrow \alpha$ and $\alpha \rightarrow \beta$ transitions occur at temperatures 186 and 1114 K, respectively. We also notice that the thermal electronic contribution to both enthalpy and entropy becomes more and more important at high temperatures for the β phase. At the 1114 K, the electronic entropy accounts for 24% of the entropy change at the $\alpha \rightarrow \beta$ transition, which is close to the experimental value 30%.[17]

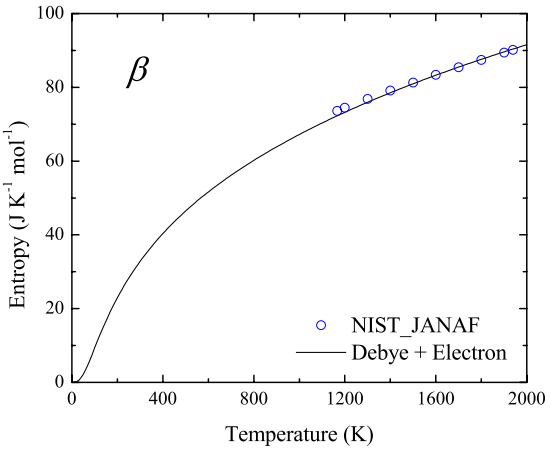

FIG. 8. (Color online) Entropy of β Ti as a function of temperature, with the experimental values from NIST-JANAF (Ref. 35) superimposed (open circles).

Zero-point energy can have a profound influence on the phase transition pressure at low temperatures.[44] In our previous work we predicted that 0 K transition pressure of $\alpha \rightarrow \omega$ to be −3.7 GPa.[14] After considering the zero-point energy, we noticed that the corresponding transition pressure increases to −1.5 GPa. For the metastable phase transitions $\alpha \rightarrow \beta$ and $\beta \rightarrow \omega$, the transition pressures at 0 K decrease to 54.2 and 95.9 GPa, respectively, compared to the predicted transition pressures of 63.7 and 106.0 GPa without considering the zero-point energy.[14] Hence, zero-point energy cannot be neglected in predicting the transition pressures of Ti at low temperatures.

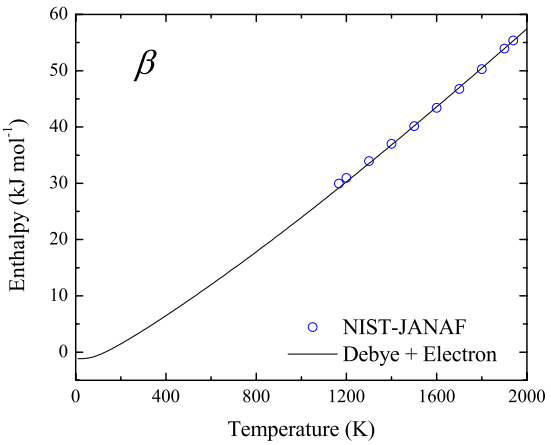

FIG. 9. (Color online) Enthalpy of β Ti as a function of temperature, with the experimental values from NIST-JANAF (Ref. 35) superimposed (open circles). The calculated enthalpies are shifted down by 8.0 kJ mol^{-1} to match the experimental data from NIST-JANAF (Ref. 35).

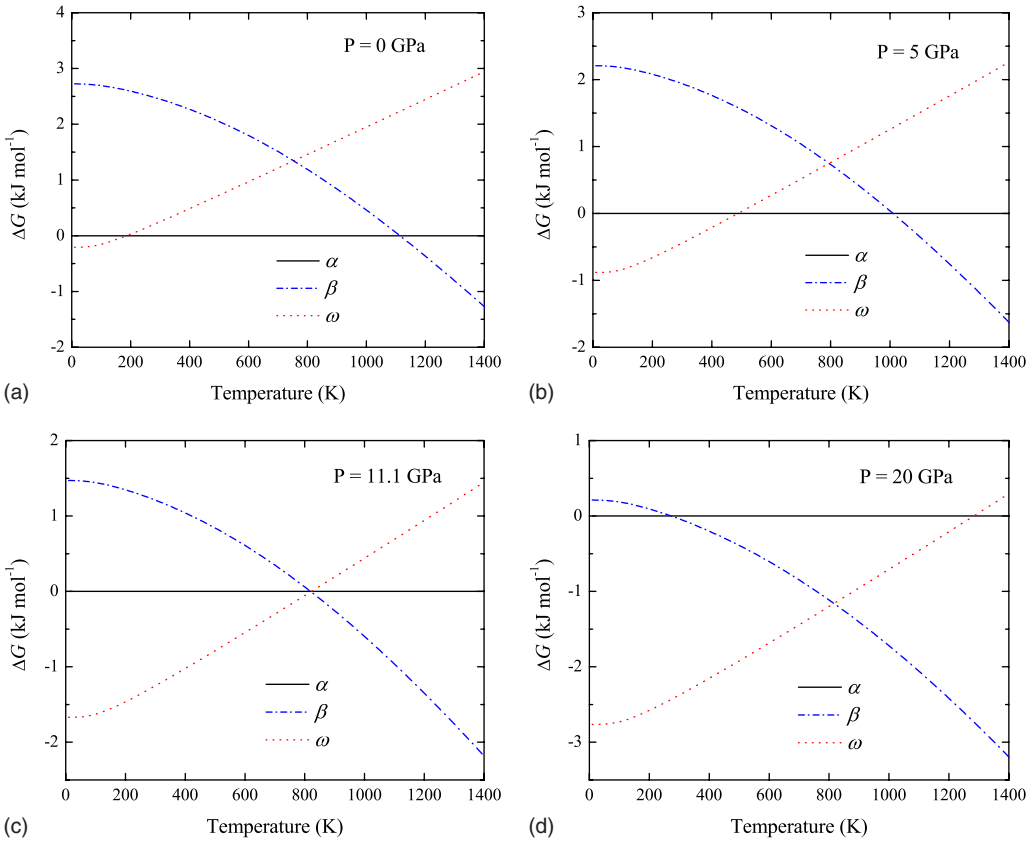

FIG. 10. (Color online) Temperature dependences of the Gibbs energy difference (ΔG) of Ti phases with respect to α at different pressures, i.e., 0, 5, 11.1, and 20 GPa.

V. SUMMARY

We studied the phonon spectra of α, β, and ω Ti using the supercell approach. The lattice vibrational energy F_{vib} was calculated based on quasiharmonic approximation from both the first-principles phonon DOS and Debye model. The thermodynamic properties of α and ω Ti were investigated using both the phonon and Debye model. It was found that the

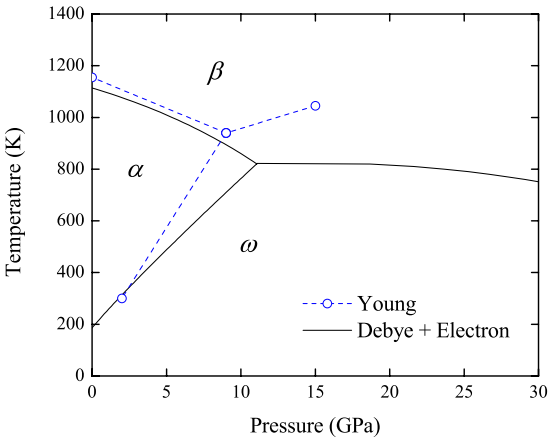

FIG. 11. (Color online) P-T phase diagram of Ti. The dashed lines connect the experimental data points are given by Young (Ref. 6); the solid lines show our predicted $\alpha \rightarrow \omega$, $\omega \rightarrow \beta$, and $\alpha \rightarrow \beta$ transition boundaries.

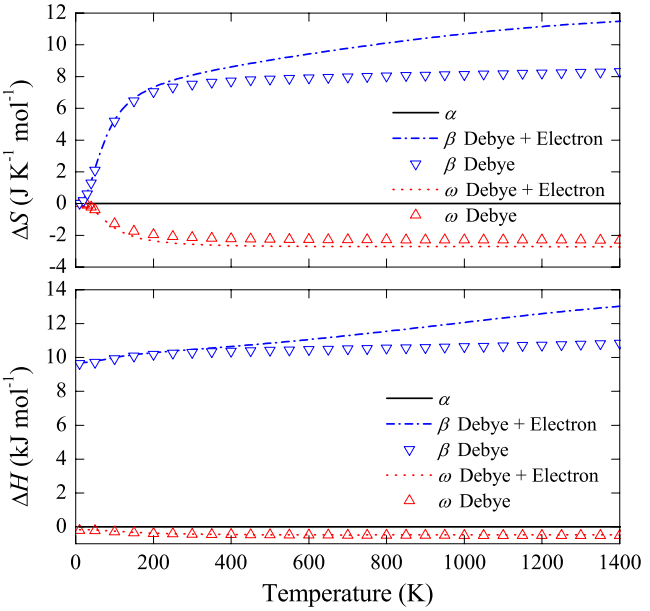

FIG. 12. (Color online) Enthalpy (ΔH) and entropy differences (ΔS) of Ti phases as a function of temperature with respect to α at ambient pressure. ΔH and ΔS differences, with and without the thermal electronic contribution, are plotted as lines and open symbols, respectively.

Debye model can well reproduce the results obtained from phonon DOS. Our predictions show that the calculated thermodynamic properties of α are in good agreement with the experiment data, except that the calculated heat capacities are somewhat higher than those of experiment at high temperatures. By comparing the calculated enthalpy of β with experiment, we found that the 0 K total energy of β calculated from simple bcc structure is too high. Shifting the total energy down by about 8 kJ mol^{-1} gives a perfect agreement of enthalpy between calculations and experiments. Based on the Gibbs energy evaluated from the Debye model as a function of pressure and temperature, we predicted the *P-T* phase diagram of α, β, and ω Ti. The calculated phase transition temperature between α and β at ambient pressure is 1114 K, comparing well with the experimental data of 1155 K. We also predicted a triple point (11.1 GPa, 821 K), which is close to the experimental data (9 GPa, 940 K). Our study showed that the entropy plays an important role in the $\omega \rightarrow \alpha$ and $\alpha \rightarrow \beta$ transitions, and the thermal electronic contribution to the $\alpha \rightarrow \beta$ transition cannot be neglected. Our calculations also indicated that zero-point energy is important in predicting the transition pressure of the Ti phases at low temperatures.

ACKNOWLEDGMENTS

This work is funded by the National Science Foundation (NSF) through Grants No. DMR-0510180 and No. IIP-0737759. First-principles calculations were carried out on the LION clusters at the Pennsylvania State University supported in part by the NSF Grants No. DMR-9983532, No. DMR-0122638, and No. DMR-0205232 and in part by the Materials Simulation Center and the Research Computing and Cyber infrastructure unit. Z.G.M. wants to thank Atsushi Togo for his valuable help and advice on using FROPHO code.

[1] H. Xia, S. J. Duclos, A. L. Ruoff, and Y. K. Vohra, Phys. Rev. Lett. **64**, 204 (1990).
[2] Y. K. Vohra and P. T. Spencer, Phys. Rev. Lett. **86**, 3068 (2001).
[3] Y. Akahama, H. Kawamura, and T. Le Bihan, Phys. Rev. Lett. **87**, 275503 (2001).
[4] H. Ogi, S. Kai, H. Ledbetter, R. Tarumi, M. Hirao, and K. Takashima, Acta Mater. **52**, 2075 (2004).
[5] V. A. Zilbershtein, N. P. Chistotina, A. A. Zharov, N. S. Grishina, and E. I. Estrin, Fiz. Metallov Metalloved. **39**, 445 (1975).
[6] D. A. Young, *Phase Diagrams of the Elements* (Uniersity of California Press, Berkeley, 1991).
[7] Y. J. Hao, L. Zhang, X. R. Chen, Y. H. Li, and H. L. He, Solid State Commun. **146**, 105 (2008).
[8] A. K. Verma, P. Modak, R. S. Rao, B. K. Godwal, and R. Jeanloz, Phys. Rev. B **75**, 014109 (2007).
[9] F. Jona and P. M. Marcus, Phys. Status Solidi B **242**, 3077 (2005).
[10] C. Bercegeay and S. Bernard, Phys. Rev. B **72**, 214101 (2005).
[11] R. Ahuja, J. M. Wills, B. Johansson, and O. Eriksson, Phys. Rev. B **48**, 16269 (1993).
[12] A. L. Kutepov and S. G. Kutepova, Phys. Rev. B **67**, 132102 (2003).
[13] S. P. Rudin, M. D. Jones, and R. C. Albers, Phys. Rev. B **69**, 094117 (2004).
[14] Z. G. Mei, S. L. Shang, Y. Wang, and Z. K. Liu, Phys. Rev. B **79**, 134102 (2009).
[15] S. A. Ostanin and V. Y. Trubitsin, J. Phys. Condens. Matter **9**, L491 (1997).
[16] R. G. Hennig, T. J. Lenosky, D. R. Trinkle, S. P. Rudin, and J. W. Wilkins, Phys. Rev. B **78**, 054121 (2008).
[17] W. Petry, A. Heiming, J. Trampenau, M. Alba, C. Herzig, H. R. Schober, and G. Vogl, Phys. Rev. B **43**, 10933 (1991).
[18] Y. Wang, Z. K. Liu, and L. Q. Chen, Acta Mater. **52**, 2665 (2004).
[19] Y. Wang, R. Ahuja, and B. Johansson, Int. J. Quantum Chem. **96**, 501 (2004).
[20] M. T. Dove, *Introduction to Lattice Dynamics* (Cambridge University Press, Cambridge, 1993).
[21] V. L. Moruzzi, J. F. Janak, and K. Schwarz, Phys. Rev. B **37**, 790 (1988).
[22] G. Kresse and J. Furthmüller, Phys. Rev. B **54**, 11169 (1996).
[23] G. Kresse and D. Joubert, Phys. Rev. B **59**, 1758 (1999).
[24] J. P. Perdew, K. Burke, and M. Ernzerhof, Phys. Rev. Lett. **77**, 3865 (1996).
[25] P. E. Blöchl, Phys. Rev. B **50**, 17953 (1994).
[26] P. E. Blöchl, O. Jepsen, and O. K. Andersen, Phys. Rev. B **49**, 16223 (1994).
[27] A. Togo, F. Oba, and I. Tanaka, Phys. Rev. B **78**, 134106 (2008).
[28] F. Birch, J. Geophys. Res. **83**, 1257 (1978).
[29] J. Z. Zhang, Y. Zhao, R. S. Hixson, G. T. Gray, L. P. Wang, W. Utsumi, S. Hiroyuki, and H. Takanori, Phys. Rev. B **78**, 054119 (2008).
[30] D. Errandonea, Y. Meng, M. Somayazulu, and D. Hausermann, Physica B (Amsterdam) **355**, 116 (2005).
[31] S. N. Vaidya and G. C. Kennedy, J. Phys. Chem. Solids **33**, 1377 (1972).
[32] C. Stassis, D. Arch, B. N. Harmon, and N. Wakabayashi, Phys. Rev. B **19**, 181 (1979).
[33] P. Souvatzis, O. Eriksson, and M. I. Katsnelson, Phys. Rev. Lett. **99**, 015901 (2007).
[34] R. Arroyave and Z. K. Liu, Phys. Rev. B **74**, 174118 (2006).
[35] M. W. Chase, *NIST-JANAF Thermochemical Tables* (American Institute of Physics, Washington, D. C., 1998).
[36] E. S. Fisher and C. J. Renken, Phys. Rev. **135**, A482 (1964).
[37] Y. S. Touloukian, R. K. Kirby, R. E. Taylor, and P. D. Desai, *Thermophysical Properties of Matter Thermal Expansion* (Plenum, New York, 1975).
[38] C. W. Kothen and H. L. Johnston, J. Am. Chem. Soc. **75**, 3101 (1953).
[39] W. Bendick and W. Pepperhoff, J. Phys. F: Met. Phys. **12**, 1085 (1982).
[40] K. D. Maglic and D. Z. Pavicic, Int. J. Thermophys. **22**, 1833 (2001).

[41] Y. Wang, S. Curtarolo, C. Jiang, R. Arroyave, T. Wang, G. Ceder, L. Q. Chen, and Z. K. Liu, CALPHAD: Comput. Coupling Phase Diagrams Thermochem. **28**, 79 (2004).
[42] V. Ozolins, Phys. Rev. Lett. **102**, 065702 (2009).
[43] Y. Wang, L. G. Hector, H. Zhang, S. L. Shang, L. Q. Chen, and Z. K. Liu, Phys. Rev. B **78**, 104113 (2008).
[44] J. Iniguez and D. Vanderbilt, Phys. Rev. Lett. **89**, 115503 (2002).